Cell Reports Medicine, Volume *5*

Supplemental information

Disruption of MerTK increases the efficacy of checkpoint inhibitor by enhancing ferroptosis and immune response in hepatocellular carcinoma

Shun Wang, Le Zhu, Tianen Li, Xinxin Lin, Yan Zheng, Da Xu, Yu Guo, Ze Zhang, Yan Fu, Hao Wang, Xufeng Wang, Tiantian Zou, Xiaotian Shen, Lumin Zhang, Nannan Lai, Lu Lu, Lunxiu Qin, and Qiongzhu Dong

Supplementary information

Disruption of MerTK Increases the Efficacy of Checkpoint Inhibitor by Enhancing Ferroptosis and Immune Response in Hepatocellular Carcinoma

Shun Wang, Le Zhu, Tianen Li, Xinxin Lin, Yan Zheng, Da Xu, Yu Guo, Ze Zhang, Yan Fu, Hao Wang, Xufeng Wang, Tiantian Zou, Xiaotian Shen, Lumin Zhang, Nannan Lai, Lu Lu, Lunxiu Qin, Qiongzhu Dong

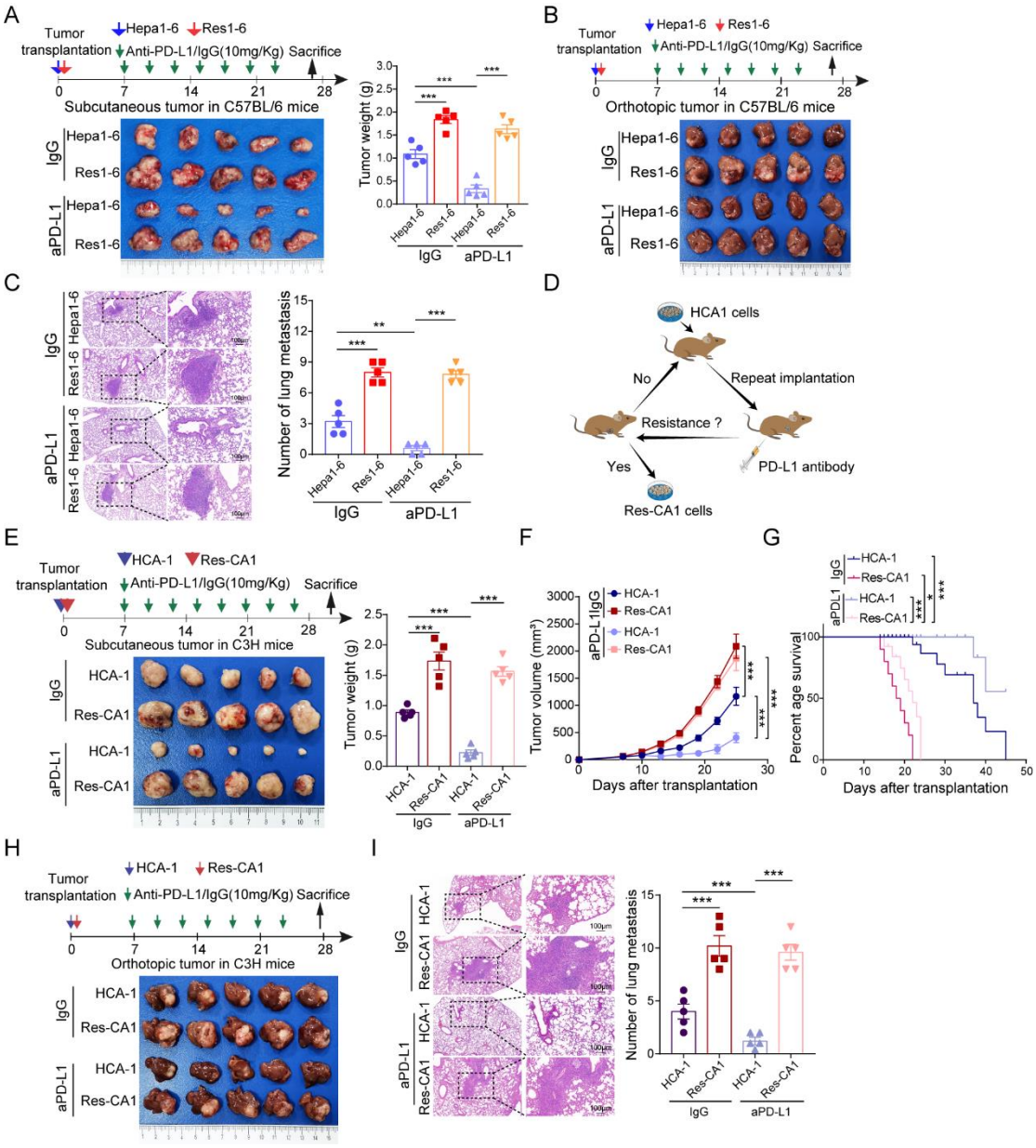

Figure S1. Establishment and identification of anti-PD-L1-resistant tumors in mice model. Related to Figure 1.

(A) Schematic illustrating the procedure of anti-PD-L1 or IgG treatment in Hepa1-6 and Res1-6 subcutaneous tumor model, and the representative images of subcutaneous tumor in different groups (left), and tumor weight statistical analysis (right). (B) Schematic illustrating the procedure of anti-PD-L1 or IgG treatment in Hepa1-6 and Res1-6 orthotopic tumor model (upper), and the final representative images (lower). (C) Representative HE staining images of lung tissues in different groups (left). Scale bar, 100 μm, and the number of lung metastasis foci statistical analysis (right). (D) Schematic illustrating the establishment of anti-PD-L1-resistant HCA1 strains in vivo. (E) Schematic illustrating the procedure

of anti-PD-L1 or IgG treatment in HCA1 and Res-CA1 subcutaneous tumor model, and the representative images of subcutaneous tumor in different groups (left), and tumor weight statistical analysis (right). (F) Statistical analysis of tumor growth curves. (G) Survival of orthotopic implantation models of HCA1 and Res-CA1 strains treated with anti-PD-L1 or IgG. (H) Schematic illustrating the procedure of anti-PD-L1 or IgG treatment (upper), and the final representative images (lower). (I) Representative HE staining images of lung tissues in different groups (left). Scale bar, 100 μm, and the number of lung metastasis foci statistical analysis (right). All results are shown as the mean ± SEM (n = 5). One- or two-way ANOVA was used to analyze the data; *$p < 0.05$, **$p < 0.01$, ***$p < 0.001$.

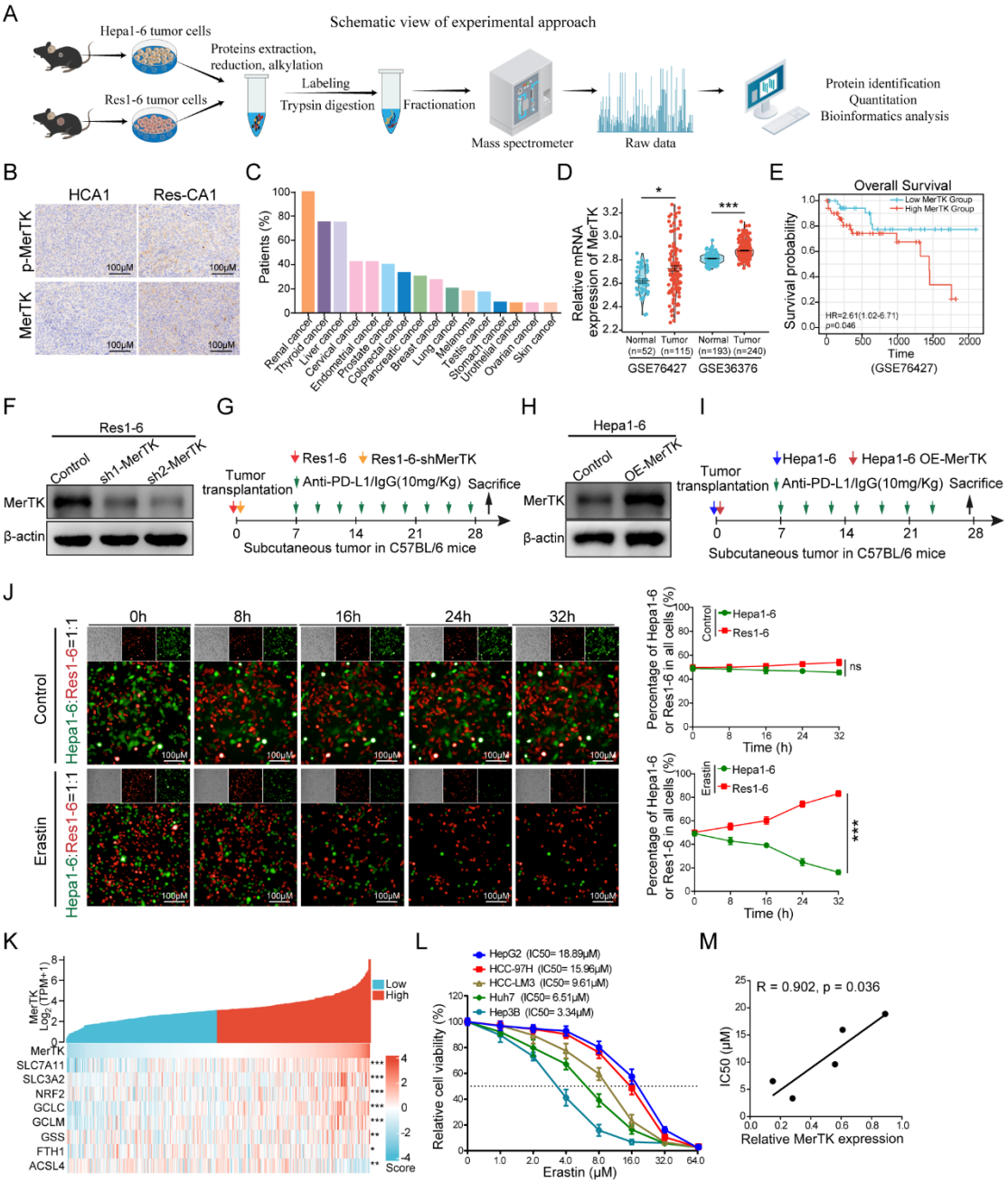

Figure S2. MerTK expression is associated with poor prognosis and positively correlated with SLC7A11 in HCC. Related to Figure 1 and Figure 2.

(A) Schematic illustrating the proteomic sequencing procedure. (B) IHC staining of p-MerTK and MerTK in HCA-1 and Res-CA1 subcutaneous tumor tissues. (C) MerTK expression level in different tumors. (D) The GEO database revealed that MerTK expression was significantly upregulated in HCC patients. The boxplot analysis showed log2 (TPM+1) on a log-scale. (E) The OS of HCC patients in GSE76427 database. (F) Identification of MerTK knockdown in Res1-6-sh-MerTK cells. (G) Schematic illustrating the procedure of anti-PD-L1 or IgG treatment in Res1-6 and Res1-6-sh-MerTK subcutaneous

tumor model. (H) Identification of MerTK over-expression. (I) Schematic illustrating the procedure of treatment in Hepa1-6 and Hepa1-6-OE-MerTK subcutaneous tumor model. (J) Cell viability of Res1-6 and Hepa1-6 strains treated with erastin (5.0 μM) in coculture condition (left) and statistical analysis of cell survival rate in each time point (right). (K) The correlation analysis between the expression of MerTK and ferroptosis related genes in HCC patients from TCGA dataset. (L) Cell viability (%) of HCC cell lines treated with erastin (0, 1.0, 2.0, 4.0, 8.0, 16.0, 32.0 and 64.0 μM). (M) The correlation between MerTK expression and Cell viability of HCC cell lines treated with erastin. All results are shown as the mean ± SEM (n = 5). One- or two-way ANOVA was used to analyze the data; *$p < 0.05$, ***$p < 0.001$.

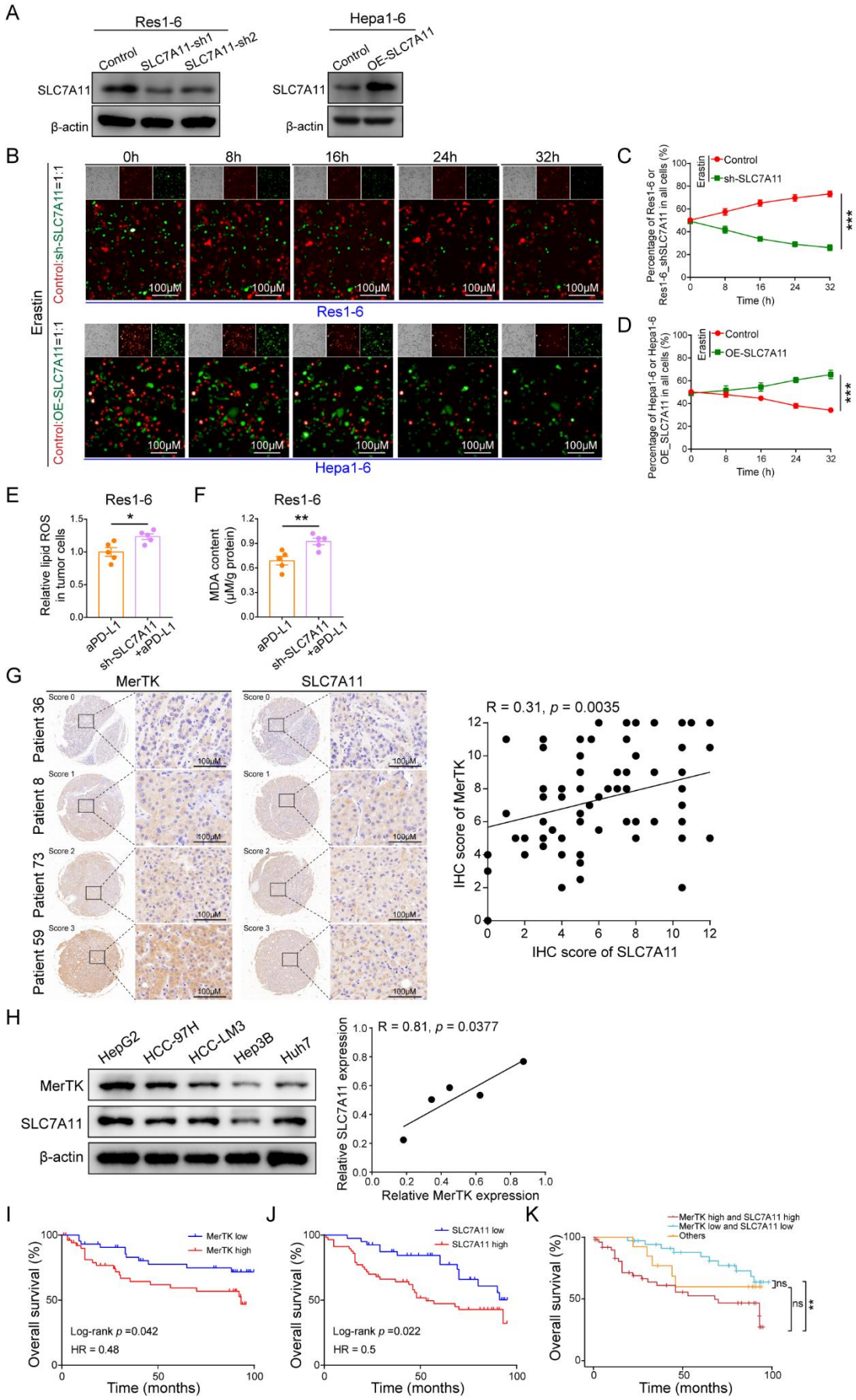
A
Res1-6
Control
SLC7A11-sh1
SLC7A11-sh2
SLC7A11
β-actin
Hepa1-6
Control
OE-SLC7A11
SLC7A11
β-actin
B
0h
8h
16h
24h
32h
Erastin
Control:sh-SLC7A11=1:1
100μM
Res1-6
Control:OE-SLC7A11=1:1
Hepa1-6
C
Erastin
Control
sh-SLC7A11
Percentage of Res1-6 or Res1-6_shSLC7A11 in all cells (%)
Time (h)
***
D
Erastin
Control
OE-SLC7A11
Percentage of Hepa1-6 or Hepa1-6 OE_SLC7A11 in all cells (%)
Time (h)
***
E
Res1-6
Relative lipid ROS in tumor cells
*
aPD-L1
sh-SLC7A11 +aPD-L1
F
Res1-6
MDA content (μM/g protein)
**
aPD-L1
sh-SLC7A11 +aPD-L1
G
MerTK
SLC7A11
Patient 36
Patient 8
Patient 73
Patient 59
Score 0
Score 1
Score 2
Score 3
100μM
R = 0.31, p = 0.0035
IHC score of MerTK
IHC score of SLC7A11
H
HepG2
HCC-97H
HCC-LM3
Hep3B
Huh7
MerTK
SLC7A11
β-actin
R = 0.81, p = 0.0377
Relative SLC7A11 expression
Relative MerTK expression
I
MerTK low
MerTK high
Overall survival (%)
Log-rank p =0.042
HR = 0.48
Time (months)
J
SLC7A11 low
SLC7A11 high
Overall survival (%)
Log-rank p =0.022
HR = 0.5
Time (months)
K
MerTK high and SLC7A11 high
MerTK low and SLC7A11 low
Others
Overall survival (%)
ns
ns
**
Time (months)

Figure S3. MerTK expression is positively correlated with SLC7A11 and poor overall survival of HCC. Related to Figure 3.

(A) Western blot analysis of SLC7A11 expression in Res1-6, Res1-6-shSLC7A11, Hepa1-6, and Hepa1-6-OE-SLC7A11 cells. (B-D) Cell viability of Res1-6, Res1-6-sh-MerTK, Hepa1-6, and Hepa1-6-OE-SLC7A11, strains treated with erastin (5.0 μM) in coculture condition (left) and statistical analysis of cell survival rate in each time point (right). (E) The statistical analysis of relative lipid ROS, and (F) MDA content in Res1-6 and Res1-6-shSLC7A11 strains treated with anti-PD-L1. (G) IHC staining of MerTK and SLC7A11 in HCC patients' (n = 98) tumor tissues (left), and pearson product-moment correlation coefficients and the *p* values are shown (right). Scale bar: 100 μm. (H) Western blot analysis of MerTK and SLC7A11 expression in human HCC cell lines (HepG2, MHCC97-H, HCC-LM3, Hep3B, Huh7) (left), and correlation analysis (right). (I-K) Overall survival curves in HCC patients with differential expression of MerTK, SLC7A11, and combinations of MerTK and SLC7A11 calculated by Kaplan-Meier analysis and compared with the Log-rank test. All results are shown as the mean ± SEM (n = 5). One- or two-way ANOVA was used to analyze the data; *p < 0.05, **p < 0.01, ***p < 0.001.

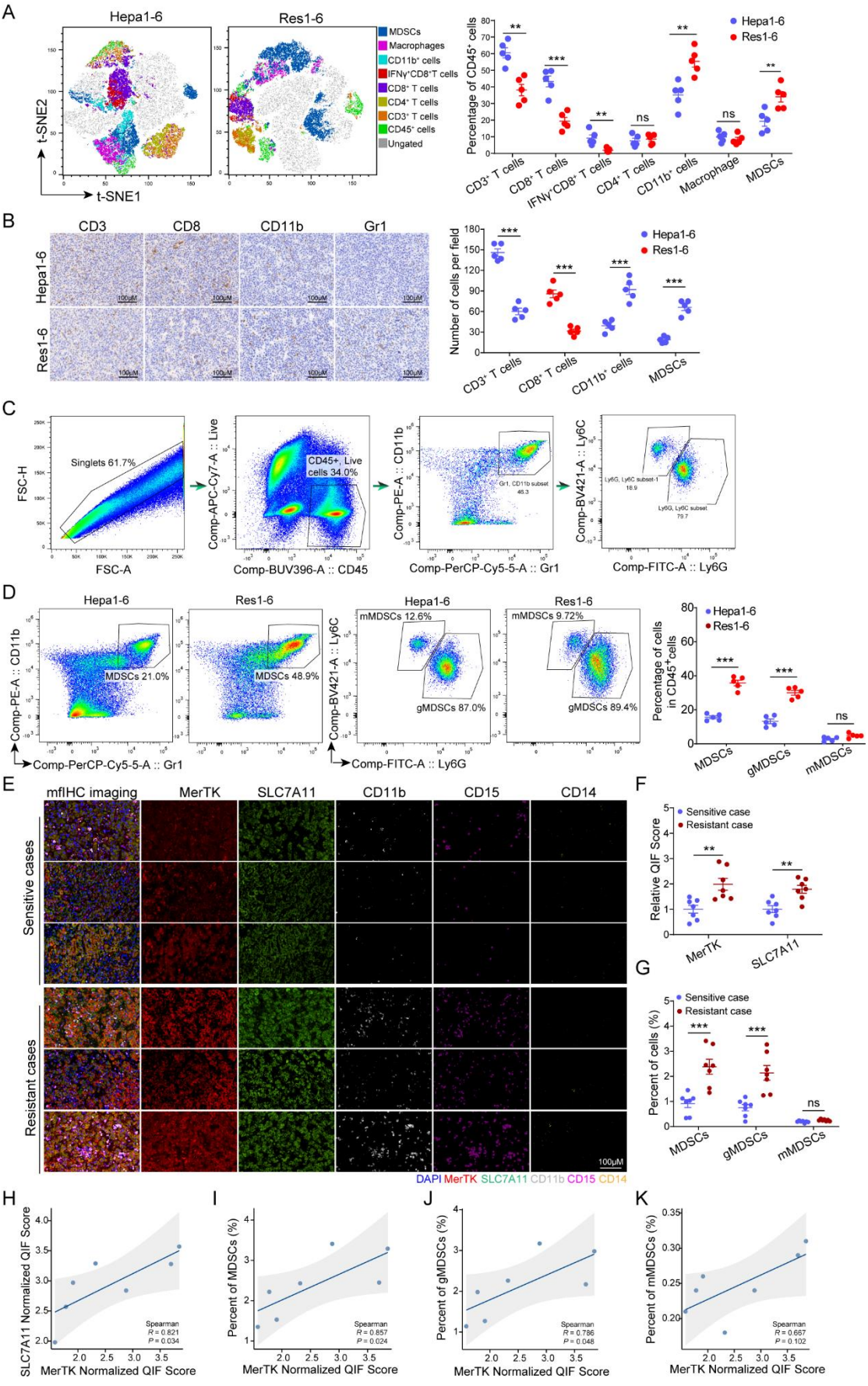
A
Hepa1-6
Res1-6
MDSCs
Macrophages
CD11b+ cells
IFNγ+CD8+T cells
CD8+ T cells
CD4+ T cells
CD3+ T cells
CD45+ cells
Ungated
t-SNE2
t-SNE1
Percentage of CD45+ cells
CD3+ T cells
CD8+ T cells
IFNγ+CD8+ T cells
CD4+ T cells
CD11b+ cells
Macrophage
MDSCs
B
CD3
CD8
CD11b
Gr1
Hepa1-6
Res1-6
Number of cells per field
C
Singlets 61.7%
FSC-H
FSC-A
CD45+, Live cells 34.0%
Comp-APC-Cy7-A :: Live
Comp-BUV396-A :: CD45
Comp-PE-A :: CD11b
Comp-PerCP-Cy5-5-A :: Gr1
Comp-BV421-A :: Ly6C
Comp-FITC-A :: Ly6G
D
MDSCs 21.0%
MDSCs 48.9%
mMDSCs 12.6%
gMDSCs 87.0%
mMDSCs 9.72%
gMDSCs 89.4%
Percentage of cells in CD45+cells
MDSCs
gMDSCs
mMDSCs
E
mfIHC imaging
MerTK
SLC7A11
CD11b
CD15
CD14
Sensitive cases
Resistant cases
100μM
DAPI MerTK SLC7A11 CD11b CD15 CD14
F
Sensitive case
Resistant case
Relative QIF Score
G
Percent of cells (%)
H
SLC7A11 Normalized QIF Score
MerTK Normalized QIF Score
Spearman R = 0.821 P = 0.034
I
Percent of MDSCs (%)
Spearman R = 0.857 P = 0.024
J
Percent of gMDSCs (%)
Spearman R = 0.786 P = 0.048
K
Percent of mMDSCs (%)
Spearman R = 0.667 P = 0.102

Figure S4. Significant increase of MDSCs and decrease of $CD8^+$ T cell infiltration observed in the tumor microenvironment of HCC that were resistant to PD-L1 blockade. Related to Figure 5.

(A) t-SNE plot of tumor-infiltrating leukocytes overlaid with col-or-coded clusters, and the frequency of clusters of the indicated immune cell subsets, including $CD3^+$ T cells, $CD8^+$ T cells, $IFN\gamma^+CD8^+$ T cells, $CD4^+$ T cells, $CD11b^+$ cells and MDSCs in Hepa1-6 and Res1-6 subcutaneous tumor model (left), and the statistical analysis (right). (B) The IHC staining representative imagines of CD3, CD8, CD11b and Gr1 from Hepa1-6 and Res1-6 subcutaneous tumors, scale bar: 100 μm (left), and the statistical analysis (right). (C) Gated strategies of Flow cytometric analysis for MDSCs, gMDSCs, and mMDSCs. (D) Flow cytometry of tumor-infiltrating MDSCs, gMDSCs, and mMDSCs in Hepa1-6 and Res1-6 subcutaneous tumors (left), and the statistical analysis (right). (E) The representative image of HCC tissue stained with MerTK (red), SLC7A11 (green), CD11b (silvery), CD15 (purple), and CD14 (golden). (F) The statistical analysis of relative QIF score of MerTK and SLC7A11. (G) The statistical analysis of percent of MDSCs, gMDSCs, and mMDSCs. (H) The correlation analysis between the expression of MerTK and SLC7A11. (I) The correlation analysis between the expression of MerTK and the enrichment of total MDSCs, (J) gMDSCs, and (K) mMDSCs. All results are shown as the mean ± SEM (n = 5). One- or two-way ANOVA was used to analyze the data; $*p < 0.05$, $**p < 0.01$, $***p < 0.001$.

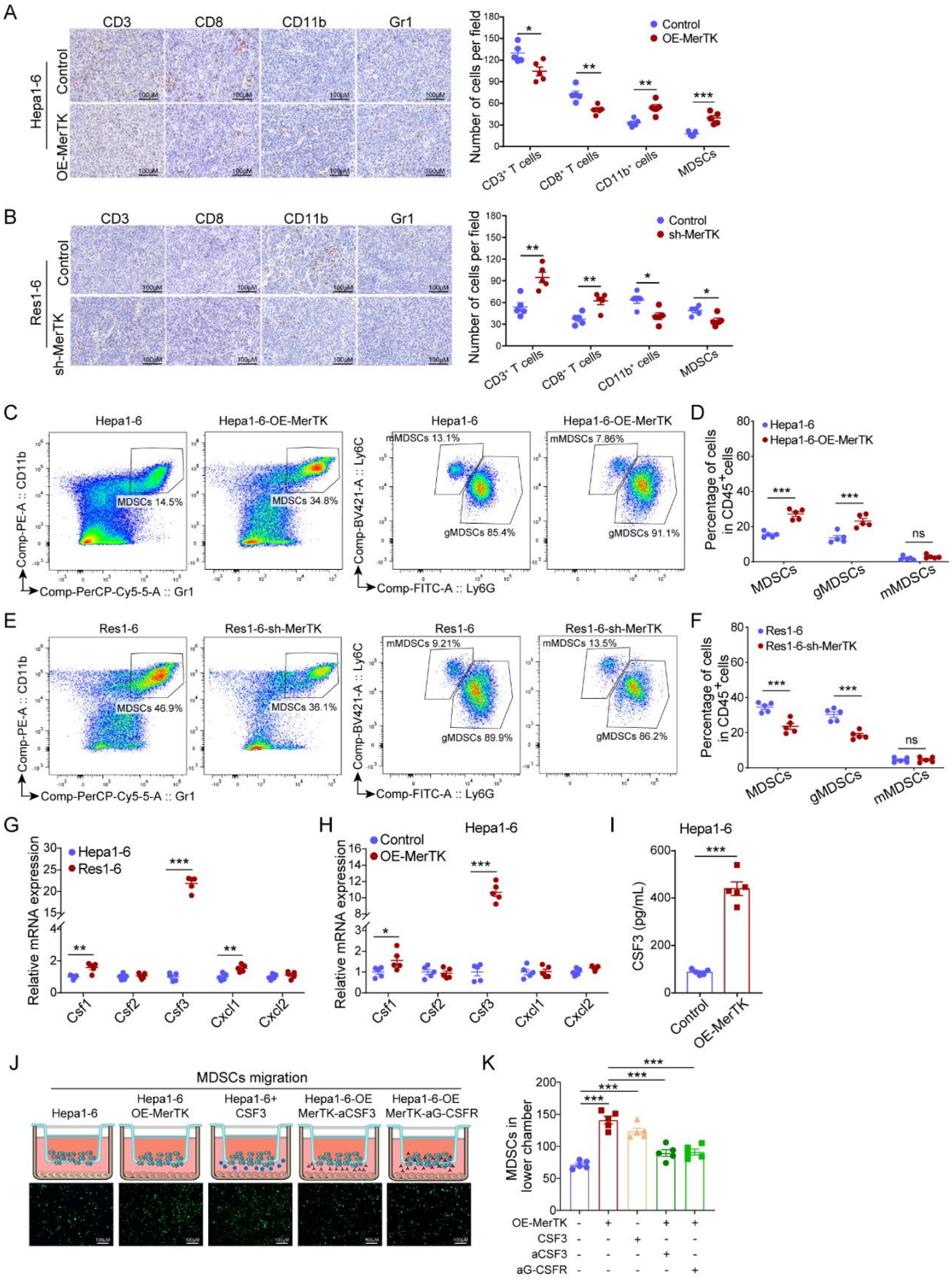

Figure S5. MerTK negatively correlates with cytotoxic CD8$^+$ T cells infiltration in HCC. Related to Figure 5.

(A-B) The IHC staining representative imagines of CD3, CD8, CD11b and Gr1 in Hepa1-6, Hepa1-6-OE-MerTK, Res1-6, and Res1-6-shMerTK subcutaneous tumor model treated with anti-PD-L1 or IgG (left), and the statistical analysis (right). (C) Flow cytometry of tumor-infiltrating MDSCs, gMDSCs, and

mMDSCs in Hepa1-6 and Hepa1-6-OE-MerTK subcutaneous tumors, and (D) the statistical analysis. (E) Flow cytometry of tumor-infiltrating MDSCs, gMDSCs, and mMDSCs in Res1-6 and Res1-6-sh-MerTK subcutaneous tumors, and (F) the statistical analysis. (G) Expression of markers associated with MDSCs chemokines (CSF1, CSF2, CSF3, CXCL1, CXCL2) in Hepa1-6 and Res1-6 cells. (H) Expression of markers associated with MDSCs chemokines (CSF1, CSF2, CSF3, CXCL1, CXCL2) in Hepa1-6 and Hepa1-6-OE-MerTK cells. (I) Supernatants were analyzed by ELISA for the levels of CSF3. (J) MDSCs were subjected to migration assays, and (K) the quantity of MDSCs in lower chamber and statistical analysis in different groups. All results are shown as the mean ± SEM (n = 5). One- or two-way ANOVA was used to analyze the data; *$p < 0.05$, **$p < 0.01$, ***$p < 0.001$.

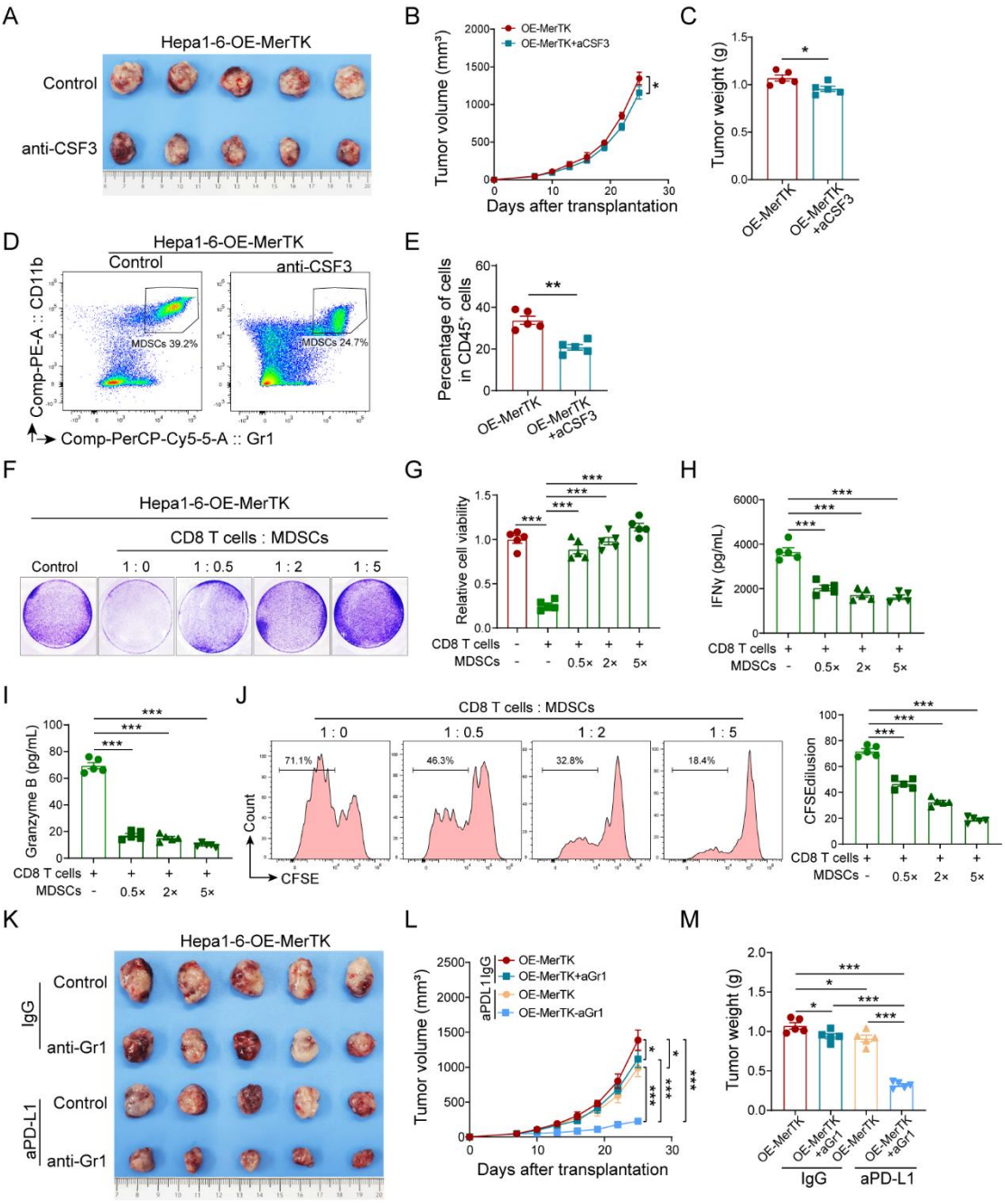

Figure S6. Depletion of MDSCs is sufficient to overcome the effects of MerTK and sensitizes anti-PD-L1 treatment efficacy. Related to Figure 5.

(A) The representative images of subcutaneous tumor in Hepa1-6-OE-MerTK and Hepa1-6-OE-MerTK treated with anti-CSF3 antibody. (B) Tumor growth curves, and (C) statistical analysis tumor weight. (D) Flow cytometry of tumor-infiltrating MDSCs in Hepa1-6-OE-MerTK and Hepa1-6-OE-MerTK treated with anti-CSF3 antibody subcutaneous tumors, and (E) the statistical analysis. (F) $CD8^+$ T cell mediated cytotoxic assays were carried out in 12-well plated and MDSCs were added into the cocultured system at graded $CD8^+$ T cells: MDSCs ratio of 1: 0, 1: 0.5, 1: 2, 1: 5. (G) The survival of Hepa1-6-OE-MerTK

cells were assessed by CCK-8 assay. (H) The coculture supernatants were analyzed by ELISA for the levels of IFN-γ and (I) Granzyme (J) $CD8^+$ T cell proliferation (CFSE-dilution) was detected by flow cytometry (left) and the quantitative analysis were presented (right). (K) The representative images of subcutaneous xenograft mouse model of Hepa1-6-OE-MerTK strains treated with anti-PD-L1, anti-Gr1 or their combination. (L) The statistical analysis of tumor growth curves. (M) The tumor weight statistical analysis. All results are shown as the mean ± SEM (n = 5). One- or two-way ANOVA was used to analyze the data; *$p < 0.05$, **$p < 0.01$, ***$p < 0.001$.

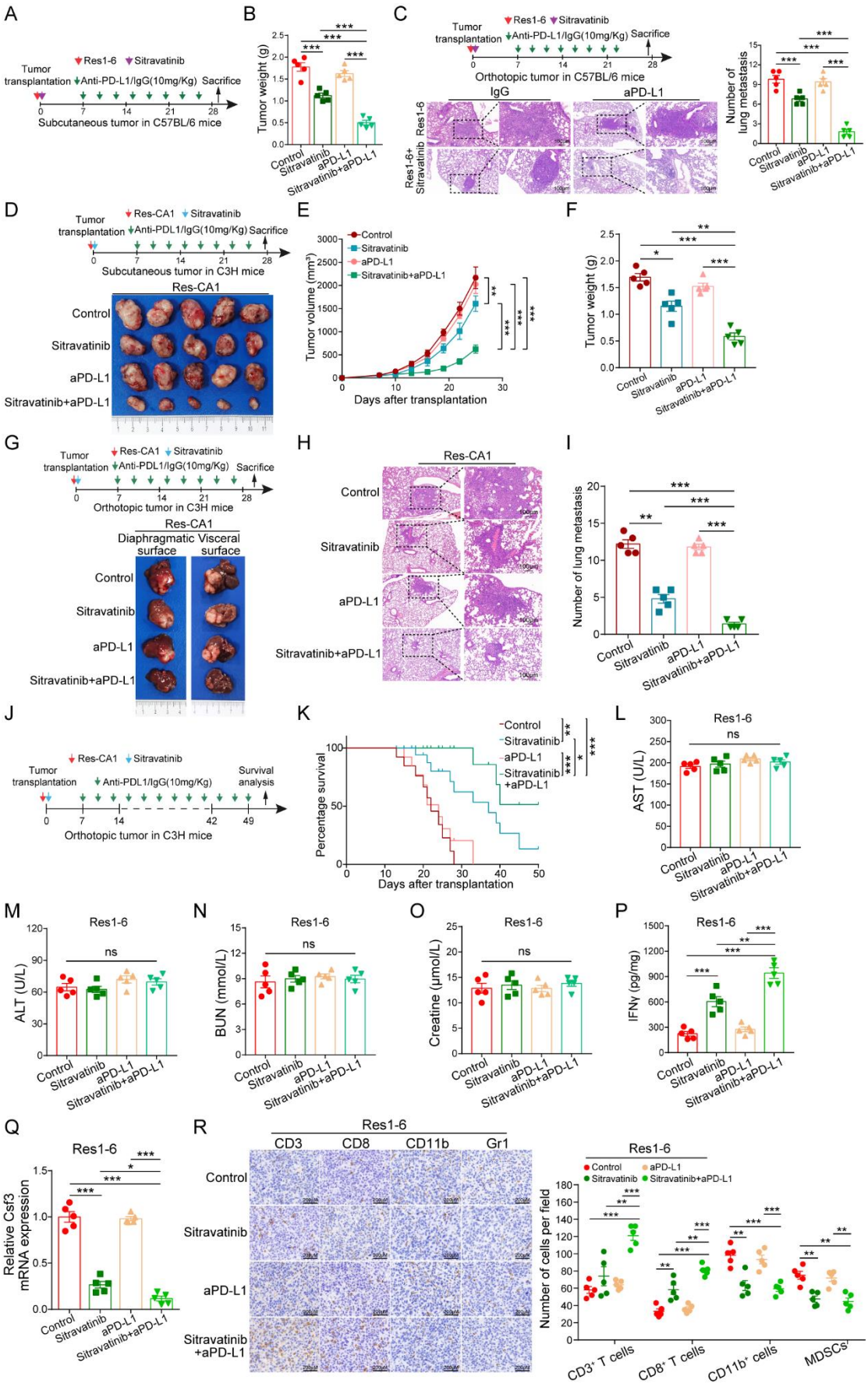
A
Res1-6
Sitravatinib
Tumor transplantation
Anti-PD-L1/IgG(10mg/Kg)
Sacrifice
Subcutaneous tumor in C57BL/6 mice
B
Tumor weight (g)
Control
Sitravatinib
aPD-L1
Sitravatinib+aPD-L1
C
Orthotopic tumor in C57BL/6 mice
IgG
aPD-L1
Res1-6
Res1-6+ Sitravatinib
Number of lung metastasis
D
Res-CA1
Subcutaneous tumor in C3H mice
E
Tumor volume (mm³)
Days after transplantation
F
G
Orthotopic tumor in C3H mice
Diaphragmatic surface
Visceral surface
H
I
Number of lung metastasis
J
Survival analysis
Orthotopic tumor in C3H mice
K
Percentage survival
L
AST (U/L)
M
ALT (U/L)
N
BUN (mmol/L)
O
Creatine (μmol/L)
P
IFNγ (pg/mg)
Q
Relative Csf3 mRNA expression
R
CD3
CD8
CD11b
Gr1
Number of cells per field
CD3⁺ T cells
CD8⁺ T cells
CD11b⁺ cells
MDSCs
ns

Figure S7. Sitravatinib in combination with anti-PD-L1 effectively show significant inhibition of anti-PD-L1-resistant strains. Related to Figure 6 and Figure7.

(A) Schematic illustrating procedure of subcutaneous tumor in Res1-6 strains were treated with IgG, sitravatinib, anti-PD-L1 or their combination. (B) The statistical analysis of tumor weight. (C) Schematic illustrating procedure of orthotopic tumor in Res1-6 strains treated with IgG, sitravatinib, anti-PD-L1 or their combination, and representative HE staining images of lung tissues in different groups (left), and the number of lung metastasis foci statistical analysis (right). (D) Schematic illustrating procedure of subcutaneous tumor in Res-CA1 strains were treated with IgG, sitravatinib, anti-PD-L1 or their combination (upper), and the representative images of subcutaneous tumor (lower). (E) The statistical analysis of tumor growth curves, and (F) the statistical analysis of tumor weight. (G) Schematic illustrating procedure of orthotopic tumor in Res-CA1 strains treated with IgG, sitravatinib, anti-PD-L1 or their combination (upper), and the representative images of orthotopic tumor (lower). (H) Representative HE staining images of lung tissues in different groups. Scale bar, 100μm, and (I) the number of lung metastasis foci statistical analysis. (J) Schematic illustrating procedure of orthotopic tumor in Res-CA1 strains treated with IgG, sitravatinib, anti-PD-L1 or their combination (left), and (K) the statistical analysis of survival curves (right). (L) Indicators of liver function aspartate aminotransferase (AST, U/L), and (M) alanine aminotransferase (ALT, U/L) in mice treated with IgG, sitravatinib, anti-PD-L1 or their combination. (N) Indicators of kidney function blood urea nitrogen (BUN, mg/dL), and (O) serum creatinine (Cr, μmol/L) in C56BL/6 mice treated with IgG, sitravatinib, anti-PD-L1 or their combination. (P) The tumor tissue homogenates were analyzed by ELISA for the levels of IFN-γ in Res1-6 subcutaneous tumor treated with IgG, sitravatinib, anti-PD-L1 or their combination. (Q) The relative Csf3 mRNA expression in Res1-6 subcutaneous tumor treated with IgG, sitravatinib, anti-PD-L1 or their combination. (R) The IHC staining representative imagines of CD3, CD8, CD11b and Gr1 in subcutaneous tumor treated with IgG, sitravatinib, anti-PD-L1 or their combination (left), and the statistical analysis (right). All results are shown as the mean ± SEM (n = 5). One- or two-way ANOVA was used to analyze the data; *$p < 0.05$, **$p < 0.01$, ***$p < 0.001$.

Table S1. Primer sequences used in the study. Related to STAR method.

Primers used for lentivirus construction		
Name	Forward Primer (FP)	Reverse Primer (RP)
SLC7A11	ATGGTCAGAAAGCCAGTTGTG	TCATAATTCTTTAGAGTCTTCTGGT
SLC7A11-sh1	CCCTGCATATTATCTCTTCAT	ATGAAGAGATAATATGCAGGG
SLC7A11-sh2	CCGGAAATCCTCTCTATGATT	AATCATAGAGAGGATTTCCGG
MerTK	ATGGTTCTGGCCCCACTGCTAC	TCACATCAGAACTTCAGAGTCTTCC
MerTK-sh1	CTACCTCCTGTTGCGTTTAAT	ATTAAACGCAACAGGAGGTAG
MerTK-sh2	CCTGTTATATTCCCGATTAAA	TTTAATCGGGAATATAACAGG
Primer used for qRT-PCR		
Name	Forward Primer (FP)	Reverse Primer (RP)
β-actin	GGCTGTATTCCCCTCCATCG	CCAGTTGGTAACAATGCCATGT
SLC7A11	AATACGGAGCCTTCCACGAG	TTGCTATCACCGACTGGCTC
MerTK	ACGTTGGTGGATACGTGCAT	CTCTTCCCACTTCTCGGCAG
Csf1	CCTTCTTCGACATGGCTGGG	GTTCTGACACCTCCTTGGCA
Csf2	CTGGCCCCATGTATAGCTGA	TCCTCCTCAGGACCTTAGCC
Csf3	CAGCCCAGATCACCCAGAATC	GCTGCAGGGCCATTAGCTTC
Cxcl1	ACTCAAGAATGGTCGCGAGG	GTGCCATCAGAGCAGTCTGT
Cxcl2	GCTGTCCCTCAACGGAAGAA	CAGGTACGATCCAGGCTTCC

Table S2. Relationship between clinicopathological features and MerTK expression in a cohort of 98 HCC patients. Related to Figure 3.

Variable		MerTK expression		*P*
		Low (n = 44)	High (n = 54)	
Gender	Female	15	24	0.298
	Male	29	30	
Age (years)	＜50	20	18	0.221
	≥50	24	36	
AFP (ng/ml)	≤20	26	23	0.104
	>20	18	31	
ALT(U/L)	≤40	24	33	0.512
	>40	20	21	
Tumor size	≤5	30	26	**0.046***
	>5	14	28	
Vascular invasion	Yes	27	38	0.348
	No	17	16	
HBsAg	Yes	36	44	0.966
	No	8	10	
Cirrhosis	Yes	32	41	0.718
	No	12	13	
Tumor capsule formation	Yes	24	30	0.921
	No	20	24	
Tumor number	Single	38	40	0.099
	Multiple	6	15	
Tumor differention	I~II	30	39	0.663
	III~IV	14	15	
TNM stage	I	35	35	0.108
	II~III	9	19	
BCLC stage	0+A	20	19	0.301
	B+C+D	24	35	

Abbreviations: HBsAg, hepatitis B surface antigen; ALT, alanine transaminase; AFP, α-fetoprotein; BCLC, Barcelona Clinic Liver Cancer staging system; HR, hazard ratio; CI, confidence interval; NA, not adopted.

Table S3. Relationship between clinicopathological features and SLC7A11 expression in a cohort of 98 HCC patients. Related to Figure 3.

Variable		SLC7A11 expression		*P*
		Low (n = 40)	High (n = 58)	
Gender	Female	19	20	0.196
	Male	21	38	
Age (years)	＜50	16	22	0.836
	≥50	24	36	
AFP (ng/ml)	≤20	25	24	**0.04***
	>20	15	34	
ALT(U/L)	≤40	27	30	0.119
	>40	13	28	
Tumor size	≤5	30	26	**0.003****
	>5	10	32	
Vascular invasion	Yes	29	36	0.283
	No	11	22	
HBsAg	Yes	32	48	0.729
	No	8	10	
Cirrhosis	Yes	29	44	0.708
	No	11	14	
Tumor capsule formation	Yes	21	33	0.667
	No	19	25	
Tumor number	Single	33	44	0.431
	Multiple	7	14	
Tumor differention	I~II	32	37	0.084
	III~IV	8	21	
TNM stage	I	33	37	**0.044***
	II~III	7	21	
BCLC stage	0+A	18	21	0.382
	B+C+D	22	37	